Synergy of van der Waals and self-interaction corrections in transition metal monoxides

Haowei Peng and John P. Perdew

Synergy of van der Waals and self-interaction corrections in transition metal monoxides

Haowei Peng[1, *] and John P. Perdew[1, 2]

[1] *Department of Physics, Temple University, Philadelphia, PA 19122, USA*
[2] *Department of Chemistry, Temple University, Philadelphia, PA 19122, USA*

Density functional theory in principle predicts correct ground-state properties for all materials. However, the rock-salt structure of MnO has been obtained only by high-level random phase approximation and diffusion Monte Carlo (DMC). Here we propose and test for MnO, FeO, CoO, and NiO that a semilocal density functional can solve this problem by properly including both self-interaction and van der Waals corrections. The importance of the latter was previously unanticipated. The MnO structural energy difference from SCAN+rVV10+U (with U from linear response) agrees well with that from DMC.

Density functional theory (DFT) has been the workhorse for computational materials design. It is a formally exact ground-state theory, and in principle predicts the correct ground-state properties even for strongly-correlated materials, with the transition-metal (TM) monoxides MnO, FeO, CoO, and NiO as the most famous exemplars. Yet, DFT with the widely-used local or semilocal approximations to the exchange-correlation energy has been greatly challenged by these materials, not only for the band gap (however see Refs. 1–3) but also for ground-state properties such as the crystal structure for MnO and CoO. Considering the vast number of TM elements in the periodic table, as well as their critical roles in functional materials related to Li-ion batteries, water splitting, oxygen evolution catalysis, etc., solving the polymorphism stability problem in a physically sound manner is of significant importance from both theoretical and technical points of views. In this work, we will identify the physics that solves this problem for the TM monoxides.

Below the Néel temperature, these four TM oxides are insulators with a slightly distorted rocksalt (RS) lattice [4] and the AF2 antiferromagnetic configuration (defined as in Ref. 5). The widely used Perdew-Burke-Ernzerhof (PBE) [6] generalized gradient approximation (GGA) underestimates their fundamental band gaps, with zero gaps for FeO and CoO. Gap underestimation in the Kohn-Sham scheme is to be expected [1]. Of greater concern is the fact that PBE wrongly predicts the zincblende (ZB) phase as the ground state for MnO and CoO [5, 7, 8]. Self-interaction correction (SIC) [9, 10], approximated by DFT+U [11–13] with an appropriate on-site Hubbard U to the d-orbit, or via the more computationally-demanding hybrid functional [14, 15] with a fraction of exact exchange, improves the band gap [1, 2, 5, 16–21], but cannot fully recover the polymorphism energetics [5, 22]. Peng and Lany [22] first tackled this problem for MnO by the high-level adiabatic connection fluctuation-dissipation theorem random phase approximation to the correlation energy (RPA)

[23–25]. The correct energy difference between RS- and ZB-MnO, $\Delta E_{ZB/RS} = E_{ZB} - E_{RS} = 131\,\mathrm{meV/formula}$ unit (f.u.), was obtained after reducing the p-d coupling in the input DFT orbitals by an external potential [22], as confirmed later by diffusion Monte Carlo (DMC) [26].

Although RPA does not provide a practical solution due to its heavy computation cost and dependence on input orbitals, the success of RPA is suggestive. Unlike PBE, RPA includes both non-local SIC and van der Waals correction (vdWC): the total energy from RPA is in analogy to the quasi-particle band structure from G0W0 [27–29], one of the state-of-the-art approaches for SIC, and vdW interaction is seamlessly included in RPA [30]. Hence, a semilocal functional, such as PBE, with proper SIC and vdWC, may improve the polymorphism energetics for TM oxides. This would facilitate material design based on heterostructural alloys [31] as in the recent tetrahedral $\mathrm{Mn}_{1-x}\mathrm{Zn}_x\mathrm{O}$ alloy ($x \sim 0.5$) for water splitting [32], where the accurate $\Delta E_{ZB/RS}$ of MnO was critical during the computational design.

We numerically test this proposal with four representative DFT flavors: the standard PBE-GGA [6], the strongly constrained and appropriately normed (SCAN) meta-GGA [33], the rev-vdW-DF2 (revDF2) vdW functional for solids [34], and the Heyd-Scuseria-Ernzerhof range-separated hybrid functional (HSE06) [15]. SIC is applied to PBE, SCAN and revDF2 via DFT+U [12], vdWC to PBE and HSE06 via the Tkatchenko-Scheffler (TS) method [35, 36], and vdWC to SCAN via the rVV10 non-local correlation [37] (a revised form of VV10 [38]). By choosing a relatively diverse group of SIC and vdWC methods and semilocal exchange-correlation functionals, we aim to demonstrate the generality and robustness of our proposal, which should still hold in the future with new (and improved) semilocal functionals and schemes for SIC [39, 40] and vdW.

All calculations were performed with the projector augmented wave method [41] as implemented in the VASP code (version 5.4.1) [42–44], with the vdW-DF [45] and rVV10 implementations [46, 47]. The energy

cutoff for the plane-wave basis is 520 eV, and converged Γ-centered Monkhorst-Pack k-meshes [48] are used for the Brillouin zone sampling. We take the magnetic configurations for the RS and ZB phases as defined in Ref. 5, and all structures are fully relaxed.

FIG. 1. The total density of states (filled shapes) and the Mn-d-projected density of states (blue curve) of δ-MnO$_2$ from (a) PBE, (b) PBE+U, (c) SCAN, (d) SCAN+U, and (e) HSE06, with the same U value of 3 eV for both PBE and SCAN.
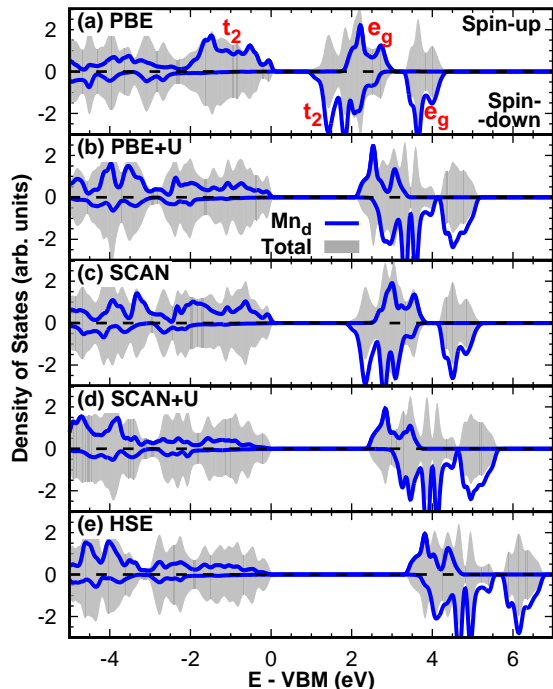
The proper amounts of SIC and vdWC are different for different DFT flavors. The vdW interaction can be roughly separated into an intermediate-range part and a long-range part. The former can be included in a semilocal functional within the exchange energy [46], being overestimated by LDA, barely included by the rev-B86b GGA [49] in revDF2, slightly included by PBE GGA, and about right in SCAN as well as the M06L [50] meta-GGAs. Accordingly, we add a large vdWC to PBE, a small vdWC to SCAN, and none to revDF2 which already includes vdW via the vdW-DF2 correlation functional [51]. A similar amount of vdWC is added to HSE06 as to PBE, as implied by a similar damping parameter of the TS method for each [36]. SCAN outperforms PBE thanks to a better description for the non-bonding overlapped electron density. Such a region is characterized by $\alpha \gg 1$, where $\alpha = \frac{\tau - \tau^W}{\tau^0}$ with τ the kinetic energy density of the valence electrons, and τ^W and τ^0 the von Weizsäcker and uniform electron gas kinetic energy densities [33, 52]. For more discussion, we refer to Ref. 46.

Figure 1 for hexagonal δ-MnO$_2$ illustrates the effects on the one-electron density of states (DOS) of the sim-

plified SICs DFT+U and HSE06: a larger and more realistic band gap (in a *generalized* Kohn-Sham scheme [1]), and a shift of the states near the conduction band minimum from t_2 (d_{xy}, d_{yz}, d_{xz}) to e_g ($d_{x^2-y^2}$, d_{z^2}) character. SCAN by itself achieves some improvement over PBE in the band gap (as in main-group solids [53]). In Fig. 1, we apply the same $U = 3$ eV for both SCAN and PBE. Comparing the DOS at the bottom of the conduction band from SCAN+U and PBE+U to that from the more-sophisticated HSE06, one can see that SCAN needs a smaller SIC correction than PBE.

TABLE I. First-principles Hubbard U parameters, in eV, for the RS- and ZB-MnO, FeO, CoO, and NiO from the self-consistent linear-response approach [54–57], for the PBE GGA and SCAN meta-GGA. The average values listed are used in the rest of this study.

	MnO		FeO		CoO		NiO	
	RS	ZB	RS	ZB	RS	ZB	RS	ZB
PBE	3.00	3.45	2.82	2.96	3.45	3.43	3.35	3.42
avg.	3.2		2.9		3.4		3.4	
SCAN	2.52	2.98	2.21	2.57	2.86	2.93	2.66	2.57
avg.	2.8		2.4		2.9		2.6	

The U parameter can be determined by using the linear-response approach [13] with self consistency [54, 55]. The actual procedure in Ref. 56 was followed, with a 64- or 72-atom supercell. The first-principles U parameters are listed in Table I for both RS- and ZB-MnO, FeO, CoO and NiO. We see that the U parameters for SCAN are generally about 0.5 eV smaller than those for PBE, consistent with the previous discussion. The average U between the RS and ZB results are used in the following calculations, and the same U parameters are assumed for PBE and revDF2.

In Fig. 2 we present the phase stability of the RS phase with respect to the ZB phase, $\Delta E_{ZB/RS}$, for MnO, FeO, CoO, and NiO, from PBE, HSE06, revDF2, and SCAN, with SIC and vdWC included as mentioned before. The experimental AF2 magnetic configuration is used for all four oxides in the RS phase, and AF1 for MnO and FeO, AF3 for CoO, and AF5 for NiO in the ZB phase are used (as defined in Ref. 5). These are also ground-state magnetic configurations from PBE and SCAN with both SIC and vdWC. Generally we find that the synergy between SIC and vdWC is critical.

MnO is the only compound among the four TM monoxides here for which the DMC result [26] provides a reliable reference. The plain PBE severely underestimates the stability of the RS phase with $\Delta E_{ZB/RS} = -244$ meV/f.u., U reduces the structural energy difference to -17 meV/f.u., and TS-vdW reduces the difference to -151 meV/f.u. The correct RS ground state is recovered only when both corrections are added, with

FIG. 2. The phase stability of the experimental ground-state rocksalt (RS) phase with respect to the zincblende (ZB) phase, $\Delta E_{ZB/RS} = E_{ZB} - E_{RS}$ in meV/f.u., from four DFT methods with self-interaction correction (via DFT+U for PBE, revDF2, and SCAN), with the vdW correction (via TS-vdW for PBE and HSE06, via rVV10 for SCAN), or with both. The DMC result [26] for MnO is indicated by a dashed line.
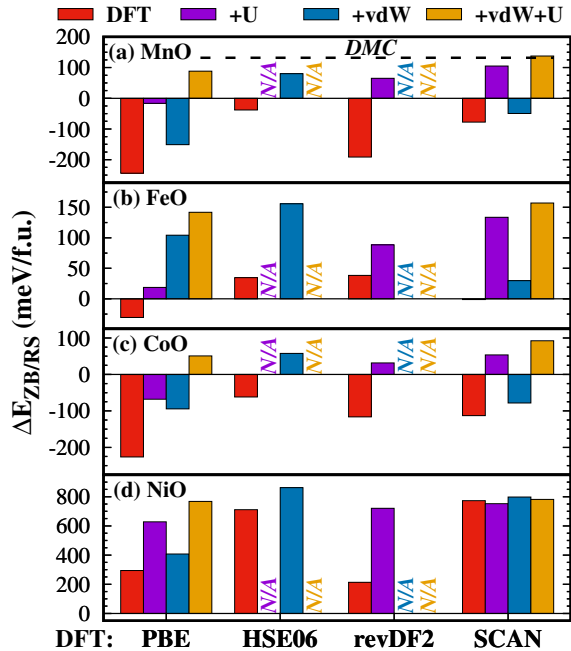
a positive $\Delta E_{ZB/RS}$ of 88 meV/f.u. The HSE06 result is very similar to the PBE+U value, and the HSE06+vdW result is very similar to PBE+U+vdW. The plain revDF2 is better than PBE, close to but slightly worse than PBE+vdW. Similarly, revDF2+U recovers the RS ground state, but with a slightly worse $\Delta E_{ZB/RS}$ than PBE+vdW+U. We attribute this to more vdW correction from TS-vdW than from revDF2, considering the fact that revDF2 slightly underestimates for molecular systems although it performs well for solids [34]. Since SCAN already includes the important intermediate-range part of vdW, we see that SCAN+U already recovers the correct ground state, and is actually better than PBE+vdW+U. Adding further the long-range vdWC from rVV10, the SCAN+vdW+U result with $\Delta E_{ZB/RS} = 135$ meV/f.u. falls within the error bar of the DMC result, 132 ± 6.5 meV/f.u.

The numerical test for MnO confirms our proposal, inspired by the RPA method, of a semilocal functional with both vdWC and SIC as a computationally efficient solution to the polymorphism energetics of the TM monoxides. In particular, SCAN+rVV10+U (SCAN+vdW+U) with a properly determined U may reach the accuracy of higher-level theory. Using the SCAN+vdW+U results as references, we see the same story in CoO, as indicated by

the similar patterns between Fig. 2(a) and (c). For FeO, PBE with either individual correction predicts the correct RS ground state, as also indicated by the plain HSE or revDF2 calculations. However the synergistic effect of the two corrections is noticeable. Another point worth noting for FeO is that the improvement of $\Delta E_{ZB/RS}$ due to the TS-vdW (123–135 meV/f.u.) is much larger than that from the DFT+U (38–49 meV/f.u.), but the reason behind this needs more detailed analysis. NiO is the only oxide of the four for which the plain PBE works well, but adding the two corrections improves the result significantly, and the PBE+vdW+U result is comparable to the SCAN+vdW+U one. We found that the corrections do not make significant changes to the SCAN result in NiO, which indicates a good error cancellation of the corrections between the RS and ZB phases.

The significant effect of vdW correction in these mainly ionically-bonded solids, with the textbook cubic lattices, is unexpected. How does this happen? The vdWC from an ion-ion pairwise model method, like TS-vdW employed here, is

$$E_{vdW} = -\frac{1}{2} \sum_{A,B} f_{damp}(R_{AB}) C_{6AB} R_{AB}^{-6}, \qquad (1)$$

where the summation runs over all possible pairs of ions with a distance of R_{AB}, and f_{damp} is the damping function. In this context, the biggest difference between the RS and ZB phases is that the RS structure has a larger coordination number (6 instead of 4) and a higher density (by about 20%). This results in a more negative vdW correction to the total energy for the RS phase than for the ZB one. In meta-GGAs, the intermediate-range

FIG. 3. The (a) electron density and (b) dimensionless α value along the nearest neighboring Mn–Mn pair, O–O pair, and Mn–O bond in the RS- and ZB-MnO from SCAN+rVV10+U.
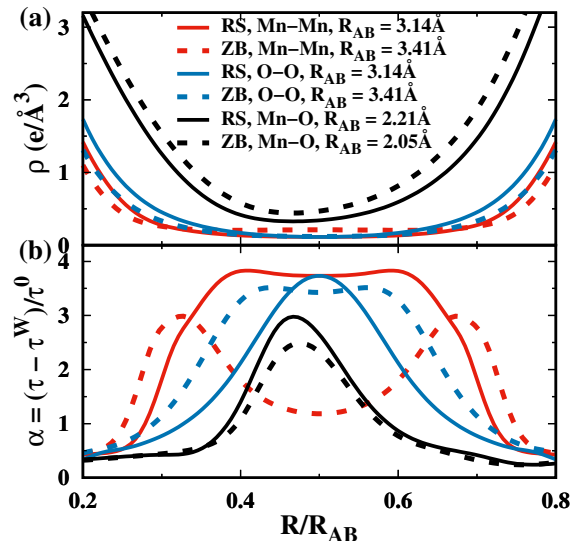
TABLE II. The calculated total energy with respect to the RS phase (ΔE in meV/f.u.), equilibrium volume (Ω_0 in Å^3/f.u.), bulk modulus (B_0 in GPa), and fundamental band gap (E_g in eV) for MnO, FeO, CoO, and NiO in both RS and ZB structures, using PBE+TS+U and SCAN+rVV10+U. The experimental data are collected in Refs. 17 and 18.

Compound		PBE+TS+U				SCAN+rVV10+U				Experiment		
		ΔE	Ω_0	B_0	E_g	ΔE	Ω_0	B_0	E_g	Ω_0	B_0	E_g
MnO	RS	**0**	21.58	156	1.8	**0**	21.71	164	2.3	21.96	$151-162$	$3.8-4.2$
	ZB	88	26.47	102	0.8	138	26.43	120	1.1			
FeO	RS	**0**	20.25	150	1.2	**0**	20.28	163	1.4	20.35	$150-180$	2.4
	ZB	142	24.34	107	0.3	157	23.15	84	0.8			
CoO	RS	**0**	19.06	184	2.3	**0**	19.08	186	2.9	19.25	180	3.6
	ZB	51	23.53	137	1.4	92	23.45	146	1.7			
NiO	RS	**0**	17.76	205	2.5	**0**	17.94	220	3.5	18.14	$166-208$	$3.7-4.3$
	ZB	768	20.55	56	0.9	782	21.16	85	1.5			

vdW interaction mainly arises from electron density with $\alpha \gg 1$ [33, 52]. In Fig. 3, we compare the electron density as well as the α value along the nearest neighboring (NN) Mn–Mn pair, O–O pair, and Mn–O bond in the RS- and ZB-MnO from SCAN+rVV10+U. Fig. 3 clearly shows that the electron density and α are significant between the ions, suggesting important vdW effects in both structures.

From the electronic structure point of view, the more negative vdW contribution for the RS phase is related to its higher ionicity than the ZB phase, partially because of the weaker p-d coupling in the former. Under the O_h symmetry in the ideal RS structure, O-p consists of a t_1 triple-degenerated state, TM-d consists of a t_2 triple-degenerated state and an e_g double-degenerated state due to the crystal field splitting, and the p-d coupling is symmetry forbidden. By contrast, under the T_d symmetry in the ideal ZB structure, O-p consists of a t_2 state, TM-d consists still of t_2 and e_g states, and p-d coupling is allowed between the t_2 states. Although the symmetry is lowered due to the magnetic configuration and lattice distortion, the chemical trend is kept. The higher iconicity in the RS phase brings in the more atom-like d states, explaining the higher α value between the Mn-Mn nearest-neighbors.

We summarize in Table II the relative energy of the ZB phase, equilibrium volume Ω_0 and bulk modulus B_0 from the Murnaghan equation of state [58] fitting, and the fundamental band gap E_g for MnO, FeO, CoO, and NiO in RS and ZB phase, with the two final corrected semilocal-level functionals PBE+TS+U and SCAN+rVV10+U. Experimental data for the RS phase are collected from Refs. 17 and 18 for comparison. The lattice volumes from both methods agree very well with the experimental values, thanks to the cancellation between the +U and +vdW corrections: DFT+U depresses the p-d coupling, and hence expands the lattice, while the attractive vdWC always compresses the lattice. The bulk moduli from both methods are also in excellent agreement

with the experimental values for the RS phase, with the SCAN+rVV10+U results systematically larger than the PBE+TS+U ones slightly. The band gaps are all nonzero, but smaller than experiment. Figures like Fig. 2, but for the volume and gap, are presented in the Supplementary Material [59]. Generally, the SCAN-based method is superior to the PBE-based one for both energetics and band gaps. Besides, SCAN is better than both PBE and LDA for localized noded orbital densities [60], relevant to the SIC of Refs. 9, 10, and 40.

In summary, we have proposed a solution, at the computational cost of a semilocal functional, to the polymorphism energetics of transition metal monoxides. This solution is inspired by the success of RPA for the correct ground state of MnO, which we attribute to the coexistence of self-interaction correction and van der Waals interactions in RPA. When such corrections are added to a semilocal functional, the correct ground-state properties are found for MnO, FeO, CoO and NiO. Unless both corrections are made together, the wrong structure is predicted for MnO and CoO. In particular, SCAN+rVV10+U, with U determined in a first-principles way, is a promising approach to reach the accuracy of DMC, as shown here for MnO and as anticipated for the other three monoxides. This should be especially helpful for the study and design of functional materials where phase transition or stability is critical, such as Li-ion battery cathode materials and heterostructural semiconductor alloys, and also for future methodology development.

* Haowei.Peng@gmail.com.

[1] J. P. Perdew, W. Yang, K. Burke, Z.-H. Yang, E. K. U. Gross, M. Scheffler, G. E. Scuseria, T. M. Henderson, I. Y. Zhang, A. Ruzsinszky, H. Peng, J. Sun, E. Trushin, and A. Görling, Proc. Natl. Acad. Sci. U. S. A. **114**, 2801 (2017).

[2] A. J. Garza and G. E. Scuseria, J. Phys. Chem. Lett. **7**, 4165 (2016).

[3] G. Trimarchi and A. Zunger, preprint.

[4] W. Roth, Phys. Rev. **110**, 1333 (1958).

[5] A. Schrön, C. Rödl, and F. Bechstedt, Phys. Rev. B **82**, 165109 (2010).

[6] J. P. Perdew, K. Burke, and M. Ernzerhof, Phys. Rev. Lett. **77**, 3865 (1996).

[7] H. X. Deng, J. Li, S. S. Li, J. B. Xia, A. Walsh, and S. H. Wei, Appl. Phys. Lett. **96**, 162508 (2010).

[8] Y. Zhang, D. A. Kitchaev, J. Yang, T. Chen, S. T. Dacek, R. A. Sarmiento-Perez, M. A. L. Marques, H. Peng, G. Ceder, J. P. Perdew, and J. Sun, submitted.

[9] J. P. Perdew and A. Zunger, Phys. Rev. B **23**, 5048 (1981).

[10] M. R. Pederson, A. Ruzsinszky, and J. P. Perdew, J. Chem. Phys. **140**, 121103 (2014).

[11] V. I. Anisimov, J. Zaanen, and O. K. Andersen, Phys. Rev. B **44**, 943 (1991).

[12] S. L. Dudarev, G. A. Botton, S. Y. Savrasov, C. J. Humphreys, and A. P. Sutton, Phys. Rev. B **57**, 1505 (1998).

[13] M. Cococcioni and S. de Gironcoli, Phys. Rev. B **71**, 035105 (2005).

[14] A. D. Becke, J. Chem. Phys. **98**, 1372 (1993).

[15] A. V. Krukau, O. A. Vydrov, A. F. Izmaylov, and G. E. Scuseria, J. Chem. Phys. **125**, 224106 (2006).

[16] J. Hugel and M. Kamal, Solid State Commun. **100**, 457 (1996).

[17] F. Tran, P. Blaha, K. Schwarz, and P. Novák, Phys. Rev. B **74**, 155108 (2006).

[18] C. Rödl, F. Fuchs, J. Furthmüller, and F. Bechstedt, Phys. Rev. B **79**, 235114 (2009).

[19] T. Bredow and A. R. Gerson, Phys. Rev. B **61**, 5194 (2000).

[20] I. P. R. Moreira, F. Illas, and R. L. Martin, Phys. Rev. B **65**, 155102 (2002).

[21] M. Alfredsson, G. D. Price, C. R. A. Catlow, S. C. Parker, R. Orlando, and J. P. Brodholt, Phys. Rev. B **70**, 165111 (2004).

[22] H. Peng and S. Lany, Phys. Rev. B **87**, 174113 (2013).

[23] D. C. Langreth and J. P. Perdew, Phys. Rev. B **21**, 5469 (1980).

[24] M. Fuchs and X. Gonze, Phys. Rev. B **65**, 235109 (2002).

[25] J. Harl and G. Kresse, Phys. Rev. Lett. **103**, 056401 (2009).

[26] J. A. Schiller, L. K. Wagner, and E. Ertekin, Phys. Rev. B **92**, 235209 (2015).

[27] L. Hedin, Phys. Rev. **139**, A796 (1965).

[28] L. Schimka, J. Harl, A. Stroppa, A. Grüneis, M. Marsman, F. Mittendorfer, and G. Kresse, Nat. Mater. **9**, 741 (2010).

[29] E. Trushin, M. Betzinger, S. Blügel, and A. Görling, Phys. Rev. B **94**, 075123 (2016).

[30] H. Eshuis, J. E. Bates, and F. Furche, Theor. Chem. Acc. **131**, 1084 (2012).

[31] A. M. Holder, S. Siol, P. F. Ndione, H. Peng, A. M. Deml, B. E. Matthews, L. T. Schelhas, M. F. Toney, R. G. Gordon, W. Tumas, J. D. Perkins, D. S. Ginley, B. P. Gorman, J. Tate, A. Zakutayev, and S. Lany, Sci. Adv. **3**, e1700270 (2017).

[32] H. Peng, P. F. Ndione, D. S. Ginley, A. Zakutayev, and S. Lany, Phys. Rev. X **5**, 021016 (2015).

[33] J. Sun, A. Ruzsinszky, and J. P. Perdew, Phys. Rev. Lett. **115**, 036402 (2015).

[34] I. Hamada, Phys. Rev. B **89**, 121103 (2014).

[35] A. Tkatchenko and M. Scheffler, Phys. Rev. Lett. **102**, 073005 (2009).

[36] N. Marom, A. Tkatchenko, M. Rossi, V. V. Gobre, O. Hod, M. Scheffler, and L. Kronik, J. Chem. Theory Comput. **7**, 3944 (2011).

[37] R. Sabatini, T. Gorni, and S. de Gironcoli, Phys. Rev. B **87**, 041108 (2013).

[38] O. A. Vydrov and T. Van Voorhis, J. Chem. Phys. **133**, 244103 (2010).

[39] C. Li, X. Zheng, A. J. Cohen, P. Mori-Sánchez, and W. Yang, Phys. Rev. Lett. **114**, 053001 (2015).

[40] Z.-H. Yang, M. R. Pederson, and J. P. Perdew, Phys. Rev. A **95**, 052505 (2017).

[41] P. E. Blöchl, Phys. Rev. B **50**, 17953 (1994).

[42] G. Kresse and J. Hafner, Phys. Rev. B **49**, 14251 (1994).

[43] G. Kresse and J. Furthmüller, Phys. Rev. B **54**, 11169 (1996).

[44] G. Kresse and D. Joubert, Phys. Rev. B **59**, 1758 (1999).

[45] J. Klimeš, D. R. Bowler, and A. Michaelides, J. Phys.: Condens. Matter. **22**, 022201 (2010).

[46] H. Peng, Z.-H. Yang, J. P. Perdew, and J. Sun, Phys. Rev. X **6**, 041005 (2016).

[47] H. Peng and J. P. Perdew, Phys. Rev. B **95**, 081105 (2017).

[48] H. Monkhorst and J. Pack, Phys. Rev. B **13**, 5188 (1976).

[49] A. D. Becke, J. Chem. Phys. **84**, 4524 (1986).

[50] Y. Zhao and D. G. Truhlar, J. Chem. Phys. **125**, 194101 (2006).

[51] K. Lee, É. D. Murray, L. Kong, B. I. Lundqvist, and D. C. Langreth, Phys. Rev. B **82**, 081101 (2010).

[52] J. Sun, B. Xiao, Y. Fang, R. Haunschild, P. Hao, A. Ruzsinszky, G. I. Csonka, G. E. Scuseria, and J. P. Perdew, Phys. Rev. Lett. **111**, 106401 (2013).

[53] Z.-H. Yang, H. Peng, J. Sun, and J. P. Perdew, Phys. Rev. B **93**, 205205 (2016).

[54] H. J. Kulik, M. Cococcioni, D. A. Scherlis, and N. Marzari, Phys. Rev. Lett. **97**, 103001 (2006).

[55] V. L. Campo Jr and M. Cococcioni, J. Phys.: Condens. Matter. **22**, 55602 (2010).

[56] M. Shishkin and H. Sato, Phys. Rev. B **93**, 085135 (2016).

[57] G. Moynihan, G. Teobaldi, and D. D. O'Regan, arXiv:1704.08076, (2017).

[58] F. Murnaghan, Proc. Natl. Acad. Sci. U. S. A. **30**, 244 (1944).

[59] See Supplemental Material at [URL will be inserted by publisher] for the equilibrium volume and band gap of MnO, FeO, CoO, and NiO by all the methods of Fig. 2.

[60] J. Sun, J. P. Perdew, Z. Yang, and H. Peng, J. Chem. Phys. **144**, 191101 (2016).